JOURNAL OF GEOPHYSICAL RESEARCH, VOL. ???, XXXX, DOI:10.1029/,

A statistical study of the Stromboli volcano explosion-quakes before and during 2002-2003 eruptive crisis

S. De Martino,[1] M. Palo,[1] G. B. Cimini,[2]

M. Palo, Dipartimento di Matematica e Informatica, Università di Salerno, Via Ponte Don Melillo, 84084 Fisciano (SA), Italy. (mpalo@unisa.it)

[1]Dipartimento di Matematica e Informatica, Università di Salerno, Via Ponte Don Melillo, 84084 Fisciano (SA), Italy

[2]Istituto Nazionale di Geofisica e Vulcanologia, Via di Vigna Murata, 605, 00143, Rome, Italy

Abstract. We study the seismic wavefield and the statistical properties of the Stromboli volcano explosions preceding and during 2002-2003 crisis. We analyze the recordings of a three-component seismometer operating since 23/05/2002 to 30/01/2003, including the first 34 days of the crisis. Before the crisis, we recognize three bell-shaped classes of spectra with maxima falling in the range 1–5 Hz. Spectral content has two main changes, the most prominent one occurring at the crisis onset when the frequency peak at ∼0.3 Hz increases in amplitude. Independent Component Analysis extracts three time-stable independent oscillations peaked at 1.1, 1.8, and 2.5 Hz, respectively, with radial and shallow polarization indicating a stable source mechanism. Energy of the explosions is log-normally distributed, except during a two-month time interval before the crisis when it shows also a higher mean value. The inter-occurrence time distributions display an homogeneous poissonian behaviour with a mean inter-time of 250 s, without changes at the crisis onset. Only swarms of explosions are not ruled by a Poisson process and display higher occurrence rates and higher energies. Finally, we depict a scheme of the crisis. A modification of the equilibrium is induced by rising magma that produces a change in the boundary conditions of the plumbing system. The escape from the equilibrium produces, at first, variations in the usual statistics of the explosions, then it leads to the lava effusion and to a pressure drop in the plumbing systems that induces a deep gas slug nucleation and the excitation of low frequencies.

1. Introduction

Volcanic activity of Stromboli cyclically goes out from its stationary behaviour to temporally get in a non-stationary one. As it is well known, the stationary behaviour is characterized by persistent tremor interrupted by low-intensity and high occurrence rate eruptions (explosions) with poissonian inter occurrence times [Chouet et al., 2003; Bottiglieri et al., 2005 and the references therein], during the non-stationary phase, effusive and paroxystic events occur, which can activate landslides and consequently tsunami. The stationary activity has been interrupted in 1975, 1985, and more recently in 2002-2003 and 2007 by eruptive crises, i.e. episodes of more vigorous activity accompanied by lava flows. Understanding how, why and when the volcanic system undergoes this transition is a challenge for volcanologists with effects not only on risk mitigation but also on the comprehension of natural systems in which low turbulence acts. Stromboli can be considered as an ideal case-type volcano to understand the processes driving the eruptions of open conduit basaltic volcanoes. Obviously, it is necessary to study the phenomenon along the whole process, i.e. the escape from the equilibrium, the non-equilibrium phase and the developing of the eruptive crisis. In fact volcanic activity at Stromboli has been investigated and monitored in the last 30 years mainly through temporary experiments, and since 2003 by a permanent seismic network.

The crisis of 2002-2003 started on 28th of December 2002 and lasted approximately six months. It consisted of an effusive phase that was punctuated, on April 5 2003, by a major explosive event (paroxysm) [Calvari et al., 2005]. After two days, a landslide occurred in the Sciara del Fuoco area (NW flank of the volcano - see Fig.1), inducing a tsunami wave

that inundated and severely damaged the coast of Stromboli Island [Bonaccorso et al., 2003; Pino et al., 2004; Tinti et al., 2005].

The 2002-2003 crisis held the attention of the volcano-related scientific community [Calvari et al., 2008], but an exhaustive seismological study is lacking. In fact, it is just during such crisis that continuous seismic monitoring started with the deployment of a permanent digital broadband network [Martini et al., 2008]. A description of the seismic activity at Stromboli before the 2002-2003 eruption is based on data provided by temporary seismic surveys [see, e.g., Dietel et al., 1994; La Rocca et al., 2000; Chouet et al, 2003; De Lauro et al., 2008].

During 2002-2003 crisis, however, a seismic station was operating for a limited time period, namely from 23/05/2002 to 30/01/2003, then including the onset of the crisis and the effusive phase, but excluding the paroxystic event. In this paper we analyze these seismic recordings. We will adopt spectral analysis, Independent Component Analysis (i.e. a decomposition method working in time-domain) and polarization analysis to characterize the seismic wavefield, while we study the statistical properties of the explosions in terms of their occurrence times and energy. This approach involves two time-scales: a short term (the duration of the explosion-quakes, i.e. tens of seconds) for the waveform analysis and a long term (hours to months) for the statistical purposes. Moreover, it allows to investigate completely the strombolian explosive activity observing the different features of the phenomenon, i.e. the seismic vibrations induced by the rising gas slugs leading to the explosions and the process ruling the slug formation.

Statistical methods in volcanology have been applied by several authors, in particular for the assessment of volcanic hazard. Stochastic and deterministic models have been

introduced to describe the occurrence times of volcanic eruptions worldwide, analyzing catalogues spanning some centuries of volcanic activity [see, e.g., De la Cruz-Reyna, 1993; Burt et al., 1994; Marzocchi et al., 2006]. In this paper we investigate the statistics of strombolian explosions and we limit our analysis to some months of activity including the onset of an eruptive crisis. A similar approach can be found in De Lauro et al. [2009] for Erebus volcano.

The paper is organized as follows. After the description of the data-set, we report the results of the spectral analysis. Then, we study the wavefield properties by the joined application of the Independent Component Analysis and of the polarization analysis to the decomposed waves. Subsequently, we characterize the macroscopic behaviour of the explosive process by estimating the energy and the inter-occurrence times and their statistical properties. A separated section is devoted to the study of swarms of explosions. Finally, we discuss the results depicting a possible scheme of the eruptive phases and reconstructing the dynamics and the style of the departure from the standard strombolian activity. We will take advantage of previous studies on 2007 crisis to sketch a general framework of the volcanic crises at Stromboli.

2. Data-set

We analyze the recordings of the seismic station operating at Stromboli in the period 23/05/2002 - 30/01/2003. The station (labeled SX15 in Fig. 1) was equipped with a three-component Lennartz 3D-5 s seismometer (LE-3D/5s) having flat frequency response in the range 0.2-40 Hz and a 24 bit RefTek 72A07 digitizer with sensitivity of 400 V/m/s. The sampling rate was equal to 50 sps [Pino et al., 2004; Cimini et al., 2006]. The station

was located about 2.5 km far from the craters in NE direction. In Fig. 1 we show the map of the island emphasizing the positions of the sensor and the craters.

Our recordings include the first 34 days of the crisis. In fact, the effusion began on December 28th, 2002, when a fissure opened at the base of the NE crater, and lasted until July 6th, 2003 [see e.g. Carapezza et al., 2004; Calvari et al., 2005; Cesca et el., 2007]. On December 30th, 2002, portions of the NW flank collapsed inducing two landslides in the area of Sciara del Fuoco which, in turn, produced a tsunami. On April 5th, 2003, a paroxysmal explosion occurred in the crater area, the largest one since 1930. The effusion has been mainly feeded by a fissure at about 550 m a.s.l. along the Sciara del Fuoco until mid-February 2003, and from a fissure formed 170 m above since then and until the end of the crisis [Carapezza et al., 2004].

We frequency filter the data to guarantee the linear response of the seismometer adopting a high-pass filter with four poles. We fix the cut-off at 0.2 Hz.

From the seismic recordings we estimate the occurrence times of the explosions. We evaluate the maximum of the signal amplitude within non-overlapping windows of 12 s and compare the maxima of two adjoining windows; we detect an explosion when both the following conditions are satisfied:

- the ratio between the maximum of the latter window and that of the former window exceeds a threshold equal to 1.8;
- the ratio between the maximum of the latter window and the standard deviation of the background seismic signal averaged upon one hour of recording exceeds a threshold equal to 4.

The optimal window length and the thresholds have been empirically estimated. We remark that we check the real occurrence of the detected explosions looking at their waveforms to exclude the picking of spurious signals as instrumental spikes or other non-volcanic signals. In this way we detect about 97000 explosions. An example of extracted time-series is shown in Fig. 2.

3. Spectral analysis

In order to evaluate the behaviour of the spectral content when the crisis is approaching, we perform a Fourier analysis of the explosions and estimated their amplitude spectra. In Fig. 3 we plot a normalized spectrogram. Each bin on the time-scale represents the averaged normalized spectra of 300 successive explosions. The graph of Fig. 3 shows that the highest spectral peaks are concentrated in bands, roughly centered at 1 Hz, 2 Hz, 2.5-4 Hz, respectively. During some periods, other bands around 0.3 Hz and 5 Hz can be distinguished, as well. From the pattern of Fig. 3 we recognize three principal variations of the basic spectral content (Phase B). The first variation occurs approximately in the period 20/06/2002 - 05/08/2002 when the band at 5 Hz appears and, at the same time, the band at 2 Hz disappears (Phase A). Another spectral change occurs at the onset of the effusion (28/12/2002) and lasts until the end of the recordings, namely the lowest spectral peak (0.3 Hz) has an abrupt increase in amplitude (Phase C). We note also two clusters of quasi-monochromatic explosions in the period 13-26/11/2002 highlighted by black boxes in Fig. 3 (Phase D). Ultimately, we recognize four classes of spectra, that we plot in Fig. 4. In fact, before the effusion, the spectra are bell-shaped with maxima mainly falling between 2 and 3 Hz. In this period, the amplitudes of the frequencies around 2 Hz may be low (Phase A) or high (Phase B) and the principal peaks are located at 1, 3, 5 Hz

(Fig. 4a) and at 1, 2, 3 Hz (Fig. 4b), respectively. After the onset of the effusion (Phase C), the envelope of the spectra becomes monotonically decreasing with the fundamental peak at 0.3 Hz (Fig. 4c). The clusters of explosions (Phase D) have their predominant peak at 2.8 Hz (Fig. 4d). In Fig. 5a-d we plot typical waveforms corresponding to the four classes of spectra.

4. Independent Component Analysis

Many decomposition methods based on the Fourier transform or on the correlation function and covariance matrix are usually adopted in seismology [see, e.g., Goldstein and Archuleta, 1987; Harris, 1991]. These methods contain the linearity as a constitutive hypothesis. When we study experimental signals extracted by monitoring natural systems displaying a non-linear behaviour (as volcanic systems), these methods can provide only a biased understanding of the systems. In such cases more complex approaches should be adopted to achieve a suitable decomposition.

Here we adopt the Independent Component Analysis (ICA). It is an entropy-based technique, which can find underlying factors or components from multivariate (multidimensional) statistical data on the basis of their statistical independence evaluated using fourth-order statistical properties [Hyvärinen et al., 2001]. Its goal is to find a linear representation of non-Gaussian data so that the components are statistically independent, or as independent as possible. ICA is based on the Central Limit Theorem which implies that the sum of two independent random variables has a distribution that is closer to Gaussian than any of the two original random variables. Hence, ICA finds one independent component maximizing its non-Gaussianity.

Let us explain in brief the mathematical setting on which ICA is based. We can suppose to have m different time-series $\mathbf{x}$ that we hypothesize to be the linear superposition of n mutually independent unknown signals $\mathbf{s}$. How $\mathbf{s}$ are mixed to compose $\mathbf{x}$ is represented by a constant unknown matrix $\mathbf{A}$. This mixing is essentially due to path, noise, instrumental transfer-functions, etc. The hypothesis is to have linear mixtures of some independent dynamical systems. If the mixing is supposed to be linear, nothing is assumed with respect to the components. Formally, the mixing model is written as $\mathbf{x} = \mathbf{As}$. In addition to the signal independence requirement, ICA assumes $m \geq n$. Under these hypotheses, the ICA goal is to obtain a matrix of separation $\mathbf{W} \simeq \mathbf{A}^{-1}$, in such a way that the vector $\mathbf{y} = \mathbf{Wx}$ is an estimate $\mathbf{y} \sim \mathbf{s}$ of the original independent signals.

The basic ICA model, summarizing, requires the following assumptions:

• all the independent components, with the possible exception of one of them, must be non-Gaussian;

• the number of the observed linear mixtures must be at least as large as the number of independent components;

• A matrix must be of full column rank.

ICA contains the following ambiguities or indeterminacies:

• we cannot determine the variance (proportional to the energy) of each independent component;

• we cannot determine the order of the independent components.

Some heuristic approaches have been proposed in literature to achieve the separation of the independent components. Among them, a good measure of non-Gaussianity is given by negentropy $\mathbf{J}$ [Hyvärinen and Oja, 2000]. The estimate of negentropy is difficult and,

in practice, some approximations must be introduced. In our case, we use the fixed-point FastICA algorithm: a computationally highly efficient method for performing the estimate of ICA [Hyvärinen et al., 2001]. Independence is here measured by the approximation of the negentropy given by:

$$J_G(\mathbf{w}) = E\{G(\mathbf{w}^T\mathbf{x})\} - E\{G(\nu)\} \tag{1}$$

where G is a suitable contrast *non-quadratic* function, $\mathbf{w}$ is a m-dimensional (weight) vector, $\mathbf{x}$ represents our mixture of signals, and $E\{\mathbf{w}^T\mathbf{x}\} = 1$, ν is a standardized Gaussian random variable. Maximizing J_G allows to find the weight vectors $\mathbf{w}_1, \ldots, \mathbf{w}_n$ and hence the independent components.

ICA has been already successfully applied to a variety of experimental signals from biology to geophysics [see, e.g., Fiori, 2003 for a review]. In particular, very interesting results were obtained analyzing the seismicity of volcanic areas [Acernese et al. 2003; De Lauro et al. 2008, 2009a, 2010], leading to the modeling of strombolian-like volcanoes as the superposition of non-linear modes of vibrating (magma-filled) cavities.

The starting point of ICA is to consider several mixtures of independent components (ICs) as input signals ($\mathbf{x}$ in the model). When more sensors are available their recordings (properly synchronized) are adopted as instantaneous mixtures. An alternative way is to consider as input the matrix composed by several reproductions of the same process. Both the approaches have been applied with success to natural systems and, in particular, to volcanic signals [Acernese et al., 2004; De Lauro et al., 2009]. Since in our case we have only one sensor, we adopt the second approach, taking as mixtures the seismic recordings of 20 explosions at our station; in this case the recordings are interpreted as different

occurrences of the same dynamical process. We analyze separately the three components of motion to take into account a possible anisotropy of the seismic wavefield. The number of mixtures is chosen on the basis of the number of ICs to be extracted. A first idea of the number of ICs is obtained by performing Principal Component Analysis (PCA) on the mixtures' matrix. This method involves a mathematical procedure that transforms a number of (possibly) correlated variables into a (smaller) number of uncorrelated variables called principal components. In detail, PCA performs the diagonalization of the covariance matrix [Hyvärinen et al., 2001]; it finds a new coordinate system of the data space and estimates the quantity of information connected with each direction by evaluating the corresponding eigenvalues. We remark that PCA is a decorrelation technique, namely it takes account of second-order statistics. In contrast, ICA is based on the much stronger criterion of statistical independence which requires higher-order correlations to be zero. We perform PCA on mixture matrices composed of 20 subsequent explosions and repeat this procedure to recover all the events without overlapping. In this way, we obtain 20 eigenvalues for each group of 20 explosions chronologically ordered. The main retained information scales with the principal components as shown in Fig. 6. It gives a first assessment of the approximation involved in the choice of the number of ICs: for instance, three or four principal components retain, respectively, the 62% and the 73% of the information.

In applying ICA we construct the mixture matrices with 20 explosions as for PCA, namely ensuring an optimal separation. As is usual in handling ICA results, among all the extracted time-series we neglect the redundant ones, that is the series with comparable waveforms and spectra [Acernese et al., 2004]. In this way we can distinguish three ICs.

In Fig. 7 (rows 1–3) we represent ICs in time and frequency domains. Each of them has a spectrum mainly peaked at one frequency. In Table 1 (column a) we summarize the frequency peak of each IC, which are labelled as IC1, IC2 and IC3, respectively. We remark that the main characteristic of these ICs does not depend on the component of motion. Moreover, they are preserved along all the groups of 20 explosions, hence these ICs can be defined as time-stable ICs. Peak frequencies of the time-stable ICs are included in the range 1-3 Hz. These values are consistent with previous estimates of strombolian ICs far from crises [Acernese et al., 2004; De Lauro et al., 2008]. The matching between the original series $\mathbf{x}$ and the reconstructed series $\bar{\mathbf{x}} = \mathbf{W}^{-1}\bar{\mathbf{y}}$ (where $\bar{\mathbf{y}}$=[IC1 IC2 IC3]) quantifies the approximation involved in considering these time-stable ICs. We calculate the cross-correlation functions between the 20 original series and the corresponding reconstructed series. The maxima of these cross-correlation functions have a mean value equal to 0.65 ± 0.1.

During particular time periods, in addition to the time-stable ICs we find two transient ICs (see Fig. 7 rows 4–5). We extract IC4 peaked at 0.3-0.4 Hz when we analyze explosions occurring in the Phase C, i.e. after the effusion onset, as described in the previous section. In addition, we extract IC5 peaked at 5 Hz during the Phase A, that is when the spectrum has an increase of the peak at 5 Hz.

5. Polarization analysis

The previous decomposition analysis gives us the basic independent oscillations that constitute our wavefield. In this section we estimate the polarization properties. A first step is to obtain the independent components with the adeguate amplitudes. This is achieved by frequency filtering the signal. The filter bands are fixed by maximizing the

cross correlation function between the ICs and filtered signals. For the estimate of the polarization our algorithm performs the diagonalization of the covariance matrix constructed using the three components of the signal (vertical, North–South, East-West), and the eigenvector corresponding to the highest eigenvalue is considered as the best estimate of the polarization vector. The algorithm returns also the rectilinearity (RL) which indicates if a linear direction of polarization exists. RL is given by $1 - \frac{\lambda_2+\lambda_3}{2\lambda_1}$, where λ_1,λ_2,λ_3 are the eigenvalues sorted by amplitude. RL value ranges between 0 and 1: $RL = 1$ when the wave is linearly polarized, and it is 0 when all the eigenvalues of the covariance matrix are equal and a preferential direction of polarization does not exist. When RL is 0.5 the polarization is planar and circular. Associating a direction of polarization to a wave is reliable only for an elliptical or linear polarization. For this reason we fixed a threshold in RL equal to 0.7. The direction of the polarization is delineated by two angles. The azimuth is the angle between the North direction and the vector measured clockwise. The dip is the angle between the z-axis and the vector. We remark that the polarization analysis can provide only a direction of oscillation, but not a sense. Hence, azimuths equal to θ and $\theta + \pi$ indicate the same polarization.

We estimate the polarization vector of the time-stable ICs along all the data-set. In detail, we calculate the polarization vector for each explosion in a moving window with length of 1.5 s for IC1 and 1 s for the IC2 and IC3 with an overlap of 90% at each step, sliding along the explosion seismogram for a duration of 20 seconds. For the three time stable ICs and for their superposition, the time-evolution of the polarization parameters along an explosion does not show strong and sudden changes or systematic patterns (see Fig. 8). The solutions oscillate around a value, supporting the hypothesis of a single

seismic phase composing the event. This behaviour is typical for properly decomposed Strombolian signals [see, e.g., De Lauro et al., 2008]. In Fig. 9 we display the distributions of the polarization parameters. They have been constructed by averaging over all the explosions and selecting the solutions with high rectilinearity ($RL \geq 0.7$). The crater area is located at 40^o-50^o from the north direction. IC1, IC2, IC3 point, respectively, towards $37^o \pm 34^o$, $47^o \pm 35^o$, $14^o \pm 30^o$. We have radial body waves affected by scattering, which becomes stronger at high frequencies and induces an error in the estimate of the polarization direction. Indeed, as it is well known, scattering and site effects can strongly influence the polarization of seismic signals in volcanic areas inducing a dispersion of the solutions and introducing preferential directions of oscillation other than the source-induced ones [see, e.g., Hellweg, 2003]. The dip angles indicates shallow oscillations, as it is typical for the strombolian explosion-quake [Chouet et al., 1997; Acernese et al., 2004]. Indeed, they are greater than 60^o in 75% of the solutions for IC1, in 93% for IC2 and in 97% for IC3. For a P-wave propagating in a homogenous medium the threshold of 60 degrees corresponds to about 2 km below the craters, i.e. the typical depth where the slugs originate [Burton et al., 2007; De Lauro et al., 2008]. We remark that if we choose frequency bands different from those of ICs we do not find a well defined polarization. For instance, signals filtered around 3.5 Hz do not show a preferential direction of oscillation (azimuth distribution is uniform), although these frequencies have not negligible amplitude in the spectra.

Finally, IC4 does not show a clear polarization direction with scattered solutions. Without a seismic array we cannot establish whether it is the effect of not-separable sources acting simultaneously or of a not-linearly-polarized signal. In fact, strombolian seismic

signals at these frequencies may be the result of a complex mixture of volcanic and non-volcanic sources which affects the wavefield and makes them not separable by ICA [De Lauro et al., 2006]. Similarly, we find scattered solutions for IC5. This result may be due to the instability of the polarization algorithm when acting on low-dimension matrices and poorly sampled signals.

6. Energy

We estimate the energy of each explosion by integrating the squared Hilbert transform of the corresponding seismic events. The edges of the integration are chosen on the basis of the amplitude of the explosion-quakes with respect to the background signal [see De Martino et al., 2004]. Fig. 10a describes the time-evolution of the mean value with the standard deviation of the energy (in log scale) computed in time-windows of 12 hours. Energy has a complex behaviour with fluctuations over many time scales. Nevertheless, we distinguish a relatively low-energy phase until October 2002 (Phase I and II in Fig. 10a). A high-energy phase occurs in the period October-December 2002, when the mean value increases of about 10% (Phase III in Fig. 10a). T-test comparing these two subsets assures that the mean values of the low-energy and high-energy phases are statistically different with a significance level of 99% or more.

In Fig. 11a-d we plot energy distributions computed in four different time intervals. Parts (a)-(c) refer to time-intervals before the crisis (Phase I, II, III, in Fig. 10a, respectively), part (d) is relative to a time-interval during the crisis (Phase IV). As it is typical for strombolian explosions, energy distributions are well described by log-normal distributions [De Martino et al., 2004]. However, in Fig. 11c - that corresponds to the time-interval during which many spikes of energy occur (Fig. 10a) - we note that the

standard deviation and the discrepancy between peak value and mean value are larger than those displayed in the other panels. This implies a sharp asymmetry of the distribution, with the values below the peak that are less probable and a deviation from the log-normal distribution. Moreover, in this time-interval the maximum of the distribution moves towards higher values confirming that the energy increases as inferred from its time-evolution.

7. Inter-times analysis

We estimate the inter-time distributions of the explosions falling within a time-window sliding along all the inter-times without overlapping. We repeat this process with different lengths of the window in the range 3-150 hours to assure a statistically relevant number of events (we chose a threshold equal to 15 events) and a good time resolution. In each case a decreasing exponential function well fit the distributions. This is confirmed also by the assessment of the variability coefficient (C_v). We remind that this value is defined as the ratio between the standard deviation and the mean value. $C_v = 0$ when the process is periodic, $C_v = 1$ for a Poisson process, and $C_v > 1$ for a clustered process [Cox and Lewis, 1966]. As an example, we have plotted the time evolution of C_v estimated in windows of 8 hours (Fig. 10b). 94% of the points are in the range $0.7 - 1.3$ and 6% are well below 1 and fall around 0.5.

In Fig. 10c we report the time-evolution of the occurrence rate estimated as the inverse of the mean inter-time in sliding window of 3 hours. Occurrence rate shows fluctuations on many time scales around a mean value of about 0.004 1/s, that corresponds to a mean inter-time of 250 s. Moreover, we evidence some oscillations in the occurrence rate with a periodicity of 3-5 days in the time-interval 15/09/02 - 05/10/02, highlighted in the figure

by the rectangle. We do not note a clear correlation of the occurrence rate with the external volcanic activity. Standard strombolian-like explosions are well described by a Poisson process [Bottiglieri et al., 2005; De Lauro et al., 2009b]. We can conclude that this feature appears also in proximity of the crisis; indeed, the occurrence times are well described by a Poisson process both before and after the crisis onset, except for some clustered events that follow different statistics. They will be analyzed in the next section.

8. Swarms

Among the explosions composing our data-set, we find also swarms of events, i.e. clusters of explosions occurring with rates significatively higher than those of the standard strombolian activity. In order to fix a threshold in the occurrence rate (λ_t) separating the swarms from the standard explosive activity, we look at their distribution. We estimate the occurrence rates as the inverse of the mean inter-time within windows of 3 hours as above. The occurrence rates are distributed as a normal function with a long tail extending at high values. The normal function implies an homogenous Poisson process, while the occurrence rates of the swarms fall in the tail and are ruled by a different process. The mean value and the standard deviation of the normal curve are equal to $\bar{\lambda} \simeq 0.004$ 1/s and $\sigma_\lambda \simeq 0.002$ 1/s, respectively; then, we impose the threshold equal to $\bar{\lambda} + 2\sigma_\lambda$. In this way the threshold is fixed to λ_t= 0.008 1/s (indicated in Fig. 10c by an horizontal line). This implies that the swarms are detectable as spikes in the time-evolution of the explosion rate. We detect the swarms estimating the explosion rate within time-windows of 3 hours. In this way we find 90 intervals where swarms occur. Putting together the consecutive 3-hour windows, we recognize 13 swarms. We note that they occur both before

and after the effusion onset. In particular, two long-lasting swarms occur in the periods 13-17/11/2002 and 23-26/11/2002, respectively.

Strombolian swarms are not only characterized by high occurrence rate. We calculate the normalized distributions of $C_v s$ estimated on the inter-times within time windows of 3 hours of all the explosions (including the swarms) and exclusively of the explosions of the swarms. C_v of the inter-times of the swarms is 0.65±0.13, whereas it is 0.83±0.13 for the overall process. The error in fitting with an exponential function (in a least square sense) the inter-time distribution of the swarms' explosions is four times the error found for the standard explosions. These results imply that a pure Poisson process may be unsatisfactory in describing the swarms.

In addition, the energy of the explosions of the swarms is about 10% higher than that of the standard activity (7.98±0.39 versus 7.23±0.26 averaging in 3-hour windows).

Fig. 12 shows the typical events composing the swarms. The explosions of the swarms have quasi-monochromatic waveforms which are stable among the events as proved by high values of the maximum of the cross-correlation function (greater than 0.7 whereas it is 0.4±0.1 on average for the first 20s of the raw standard explosions). Spectra are mostly peaked at 2.8 Hz (Fig. 12a,b), but swarms occurring after the effusion onset may contain also other quasi-monochromatic events with higher spectral content (4-5 Hz) (Fig. 12c,d). ICA applied on the swarms extract two quasi-monochromatic ICs peaked at 2.8 Hz or at 4-5 Hz which, in practice, match the original signals, suggesting a low-dimension dynamical system as source mechanism. These ICs differ from IC3 and IC5 for their different waveforms, although they share common spectra. The simple and similar waveforms of swarms' explosions suggest a very stable source mechanism

potentially connected to a direct imprint of the gas slug vibrations (see., e.g., [Vergniolle et al., 1996]).

We assess the polarization of the swarms by computing the polarization vector of the signals frequency filtered between 1 and 4 Hz and isolating the time periods of the swarms. The filter is adopted to isolate the frequency content of the swarms. We exclude from the analysis the swarms with frequency content in the range 4-5 Hz for the instability of the algorithm at these frequencies. Azimuth solutions are normally distributed with mean value equal to $18^o \pm 20^o$, whereas for the standard explosions (considering IC3 that has similar frequencies) we obtain $16^o \pm 31^o$. Hence, within the error the polarization vector of the swarms points towards the craters (as for the normal explosions) but with less dispersed azimuths. In addition, 89% of dip solutions are grater than 80^o, whereas this fraction ranges from 68% to 80% for the three time-stable ICs of the normal explosions, indicating very shallow oscillations.

Summarizing, the explosions of the swarms differ from the usual explosive activity for some features:

- high occurrence rate;
- low C_v of the inter-times;
- high energy;
- high-frequency and quasi-monochromatic waveforms;
- very low-dimensional dynamical system.

9. Discussion and conclusions

We have analyzed the seismic signals of the only three-component station operating at Stromboli volcano in the period 23/05/2002-30/01/2003, including the first 34 days of the 2002-2003 crisis, which started on 28th of December 2002. We have studied the seismic wavefield and the statistical and macroscopic features of the strombolian explosions along all the data-set in order to characterize the transition from the standard strombolian activity to the exceptional eruptive events. Strombolian explosions persist during the crisis and the time evolution of their wavefield and occurrence statistics can reveal when the crisis is approaching. In the following we summarize the experimental evidences:

• The spectral analysis shows that the frequency bands associated to the explosions undergo two changes, the most evident one occurring at the effusion onset when the lowest spectral peak ($\sim$ 0.3 Hz) becomes dominant implying a decreasing envelope. Before the crisis the spectrum is bell-shaped and we roughly sketch two classes of spectra: one with peaks at 1, 3, 5 Hz and the other with peaks at 1, 2, 3 Hz;

• We decompose the explosions by Independent Component Analysis in three time-stable signals well characterized in frequency and with peaks at 1.1 Hz, 1.8 Hz, 2.5 Hz, respectively. These ICs show radial and shallow polarization along all the data-set. Two further ICs are extracted only during some phases at 0.3 Hz and 5 Hz, but the instrumental setting makes very difficult to infer their polarization;

• Energy has a complex pattern with strong fluctuations and a not clear correlation with the external volcanic activity. The distributions maintain a substantial log-normal behaviour. A departure from this statistics occurs before the crisis when the mean value grows and the distribution have a sort of "flattening";

• Inter-time distributions display an homogenous poissonian behaviour without changes at the crisis onset. Occurrence rate has a mean value equal to 0.004 $1/s$ and normally distributed fluctuations. We do not observe sharp changes when the crisis starts;

• Swarms of explosions occur before and after the crisis onset and represent numerically about the 4% of the whole ensemble of events. Their principal differences from the normal explosions are: higher occurrence rate, a non-Poissonian behaviour of the occurrence times, higher energy, high-frequency and quasi-monochromatic spectral content, very shallow (and radial) polarization.

The waveform analysis indicates a quite stable source mechanism of the strombolian explosions developing compressive waves, even when the crisis is approaching. This can be interpreted as a substantially stable plumbing system and explains why the standard activity can resume after the crises. On the other hand, the fluid phases undergo a change of their thermodynamic state inducing variations in the emission and the occurrence style of the explosions and on their statistical properties. Nevertheless, the scheme of 2002-2003 eruptive crisis of Stromboli looking at seismological observations appears quite complex and we do not find a trivial relation between the crisis and the seismic parameters.

A departure from the standard statistics starts about two months before the crisis onset, detectable by a change of energy distribution and the presence of very high and non-Poissonian occurrence rates. When energy distribution changes, there is a simultaneous increase of the mean energy. In this phase occur one-half of the total number of swarms including two long-lasting ones.

We observe a decreasing spectral envelope after the crisis onset (Phase C), whereas it is bell-shaped during the standard strombolian activity [De Martino et al., 2004]. In the

theory of the vibrating cavities, a change of the vibrating structure has a direct connection with a change of the spectrum shape [see e.g. Fletcher, 1999]. In detail, a cylindrically-symmetric vibrating structure induces a decreasing spectrum [De Lauro et al., 2007 and reference therein]. In this scheme, the change of the spectrum at the crisis onset could represent the effect of a cylindrically-symmetric vibrating structure whose fundamental mode is at 0.3 Hz. The change of conditions inside the volcano when the effusion starts (i.e. a different height of the degassing layer) could induce the excitation of a bigger volcanic structure, neglecting local inhomogeneities. However, at these frequencies volcanic and non-volcanic sources (micro-seismic noise) may act simultaneously at Stromboli [De Lauro et al., 2006]. In order to discriminate between the two sources, we have compared the spectra of SX15 with that of a seismic station installed in the same period on the island of Alicudi [Cimini et al., 2006], in the Aeolian Archipelago, 80 km far from Stromboli. At the station of Alicudi, we have not found an increase of the low frequencies when the crisis starts, suggesting that a non-volcanic source as a storm can be discarded.

Another spectral change occurs about six months before the crisis onset (Phase A). This effect is directly interpretable as a change of the boundary conditions (from open-open to open-close) of a suitable vibrating structure as the volcanic conduit. Some authors have hypothesized a "choking" at some height induced by rising magma connected to 2007 crisis on the basis of SO2 emission and strain measurements [Burton et al., 2009; De Martino et al., 2010]. A similar mechanism can be advocated also for the observed spectral change. Nevertheless, this chocking appears as a transient condition because after about 40 days the previous spectrum is recovered. Moreover, this condition does not lead directly to the crisis, which occurs only after some months. This may be imputed to a

"weak" choking (induced, for example, by slow or not continuous magma feeding) that allows to be removed and to temporarily recover the stationary conditions.

Seismic swarms may be considered as a common element that characterizes the non-equilibrium phases of Stromboli volcano. Their shallow polarization suggests a very surficial degassing layer. Statistics of the swarms let us suppose that the dynamics of the exsolution and/or aggregation of the gas slugs should differ from the nucleation mechanism responsible of the standard strombolian activity. It could reflect an instability of magma-gas rheology during the non-equilibrium phase that, in turn, could represent a response to a rapid variation of the pressure within the volcanic conduit. In this scheme, the oscillations in the occurrence rate with a periodicity of 3-5 days that we observe in the time-interval 15/09/02 - 05/10/02 and that introduce the occurrence of many swarms could represent the beginning of this instability.

Some authors have analyzed the seismicity at Stromboli volcano during the crisis of 2007 and have found a general increase of the energy and of the explosive occurrence rate before the crisis onset [Scandone et al., 2009]. In particular, an analysis of the explosions of Stromboli before and during 2007 crisis looking at their spectral content, energy and occurrence times is reported in De Martino et al. [2010], Palo et al. [2010]. The results indicate a well defined seismic pattern which can be summarized as follow:

- inter-times are poissonianly distributed, except for swarms;
- spectra change from a bell shape to a decreasing one having the fundamental frequency at 0.3 Hz when the crisis starts;
- occurrence rate increases when the crisis starts;
- swarms occur only during the crisis;

• energy is log-normally distributed until the crisis onset, with an increase of the mean value when the crisis is approaching;

• energy loses gaussian behaviour when the crisis starts;

The authors detect also a possible precursor 20 days before the crisis, that is a modulation with a period of 3 days of the amplitude of the explosions, that was studied by analyzing the recordings of both a seismometer and a dilatometer. This signal is followed by an increase of the mean value of the energy which, in turn, introduces the crisis. The oscillations we have found in the occurrence rate before 2002-2003 crisis onset have a similar frequency content. Unfortunately, the lacking of an instrument suitable to detect these frequencies does not allow us to quantitatively sustain the hypothesis of such a type of precursor.

We can infer that both 2002-2003 and 2007 crisis show the response to rising magma in the seismic observations. During these crises, approximately the same amount of lava has been emitted [Landi et al., 2009], but the duration of 2002-2003 crisis is six times longer than that of 2007 eruption. This evidence lets us suppose very different velocities of magma ascent inducing low or fast variations of the internal state. It means that in 2007 there is a short transitory phase, whereas in 2002 the transitory phase is long allowing a smooth response of the system. This could explain why we note different "precursors" with different timing in the two cases and why in 2007 the effusion, the swarms and the occurrence rate increase do occur simultaneously, while in 2002-2003 do not. All these phenomena may be interpreted as the response of the volcano to restore the equilibrium condition perturbed by the injection of new magma.

Taking into account analogies and differences between the two crises, we depict a possible scenario of the phases involved before and during the crises of Stromboli volcano, starting from the framework proposed in De Martino et al. [2010]:

1. magma injection: A modification of the equilibrium conditions in the plumbing system is induced by rising magma some months before the crisis. This phenomenon is detectable as a modulation of the amplitude (2007) or a frequency change (Phase A in 2002-2003) of the explosions;

2. transitory phase: a first soft response of the system is an increase of energy. In 2007 it is the unique effect and the log-normal behaviour is preserved. In 2002-2003 the energy increase is accompanied by swarms and log-normality is lost (Phase III) suggesting that the departure from the equilibrium is already begun;

3. crisis: the system is completely out of equilibrium. In 2007 there is a strong response involving simultaneously the effusion, an overall increase of the occurrence rate of the explosions, the occurrence of swarms and the modification of the usual log-normal distribution of the energy. In 2002-2003 the response is soft: during the effusion the occurrence rate does not increase and the energy distribution recovers its log-normal shape (Phase IV). In both the cases, an overall pressure decrease in the plumbing systems induces a deep gas slug nucleation, with the excitation of low frequencies during the slug ascent (Phase C).

References

Acernese, F., A. Ciaramella, S. De Martino, R. De Rosa, M. Falanga. and R. Tagliaferri (2003), Neural networks for blind-source separation of Stromboli explosion quakes, *IEEE*

Trans. Neural Netw., 14, 167-175.

Acernese, F., A. Ciaramella, S. De Martino, M. Falanga, C. Godano, R. Tagliaferri (2004), Polarisation analysis of the independent components of low frequency events at Stromboli volcano (Eolian Islands, Italy), *J. Volc. Geotherm. Res., 137*, 153-168.

Bonaccorso, A., S. Calvari, G. Garfí, L. Lodato, and D. Patané (2003), Dynamics of the December 2002 flank failure and tsunami at Stromboli volcano inferred by volcanological and geophysical observations, *Geophys. Res. Lett., 30(18)*, 1941, doi:10.1029/2003GL017702.

Bottiglieri, M., S. De Martino, M. Falanga, C. Godano, M. Palo (2005), Statistics of inter-time of Strombolian explosion-quakes, *Europhys. Lett.,72*, 493-498.

Burt M. L., G. Wadge and W. A. Scott (1994), Simple stochastic modeling of the eruption history of a basaltic volcano: Nyamuragira, Zaire. *Bull. Volcanol., 56*, 87–97.

Burton, M., P. Allard, F. Muré, A. La Spina (2007), Magmatic gas composition reveals the source depth of slug-driven Strombolian explosive activity, *Science,317*, 227-230.

Burton M.R., T. Caltabiano, F. Muré, G. Salerno, D. Randazzo (2009), SO2 flux from Stromboli during the 2007 eruption: Results from the FLAME network and traverse measurements, *J. Volc. Geotherm. Res.*, 182, 214-220.

Calvari, S., L. Spampinato, L. Lodato, A. J. L. Harris, M. R. Patrick, J. Dehn, M. R. Burton and D. Andronico (2005), Chronology and complex volcanic processes during the 2002-2003 flank eruption at Stromboli volcano (Italy) reconstructed from direct observations and surveys with a handheld thermal camera, *J. Geophys. Res., 110*, B02201, doi:10.1029/2004JB003129.

Calvari, S., S. Inguaggiato, G. Puglisi, M. Ripepe, and M. Rosi (2008), The Stromboli Volcano: an integrated study of the 2002–2003 eruption introduction, in *The Stromboli Volcano: An integrated study of the 2002–2003 Eruption*, S. Calvari, S. Inguaggiato, G. Puglisi, M. Ripepe, and M. Rosi eds., AGU Geophysical Monograph Series, 182, 1–3.

Carapezza , M. L., S. Inguaggiato, L. Brusca, and M. Longo (2004), Geochemical precursors of the activity of an open-conduit volcano: The Stromboli 20022003 eruptive events, *Geophys. Res. Lett., 31*, L07620, doi:10.1029/2004GL019614.

Cesca, S., T. Braun, E. Tessmer, T. Dahm (2007), Modelling of the April 5, 2003 Stromboli (Italy) paroxysmal eruption from the inversion of broadband seismic data, *Earth plant. Sci. Lett., 261*, 164-178.

Chouet A. B. (1996), Long-period volcano seismicity: its source and use in eruption forecasting, *Nature, 380*, 309–316, doi:10.1038/380309a0.

Chouet, B., G. Saccorotti, M. Martini, P. Dawson, G. De Luca, G. Milana, and R. Scarpa (1997), Source and path effects in the wave fields of tremor and explosions at Stromboli Volcano, Italy, *J. Geophys. Res., 102(B7)*, 15,129-15,150, doi:10.1029/97JB00953.

Chouet B.A., P. Dawson, T. Ohminato, M. Martini, G. Saccorotti, F. Giudicepietro, G. De Luca, G. Milana and R. Scarpa (2003), Source mechanism of explosions at Stromboli determined from moment tensor inversions of very-long-period data, *J. Geophys. Res, 108(B1)*,2019.

Cimini, G.B., P. De Gori and A. Frepoli (2006), Passive seismology in southern Italy: the SAPTEX array, *Annals of Geophysics, 49 (2/3)*, 825–840.

Cox D. R. and P. A. W. Lewis, *The Statistical Analysis of Series of Events*, Methuen and Coltd, London, 1966.

De La Cruz-Reyna, S. (1993), Random patterns of occurrence of explosive eruptions at Colima Volcano, Mexico, *J. Volc. Geotherm. Res., 55*,(1-2),51-68.

De Lauro, E., S. De Martino, M. Falanga, M. Palo, and R. Scarpa (2005), Evidence of VLP volcanic tremor in the band [0.2–0.5] Hz at Stromboli volcano, Italy, *Geophys. Res. Lett., 32*, L17303, doi:10.1029/2005GL023466.

De Lauro, E., S. De Martino, M. Falanga, M. Palo (2006), Statistical analysis of Stromboli VLP tremor in the band [0.1–0.5] Hz: some consequences for vibrating structures, *Nonlin. Processes Geophys., 13*,393–400.

De Lauro E., S. De Martino, E. Esposito, M. Falanga, E. Tomasini (2007), Analogical model for mechanical vibrations in flue organ pipes inferred by independent component analysis, *J. Acoust. Soc. Am., 122*,4,2413–2424.

De Lauro, E., S. De Martino, E. Del Pezzo, M. Falanga, M. Palo and R. Scarpa (2008), Model for high frequency Strombolian tremor inferred by wavefield decomposition and reconstruction of asymptotic dynamics, *J. Geophys. Res., 113*,B02302,doi: 10.1029/2006JB004838.

De Lauro E., S. De Martino, M. Falanga and M. Palo (2009a), Decomposition of high-frequency seismic wavefield of the Strombolian-like explosions at Erebus volcano by independent component analysis, *Geophys. J. Int., 177*, 1399-1406, 10.1111/j.1365-246X.2009.04157.x

De Lauro, E., S. De Martino, M. Falanga, M. Palo, R. Scarpa (2009b), Strombolian-Like Volcano Activity: a Common Macroscopic Behaviour, *International Journal of Modern Physics B,23*,28–29,5543–5552.

De Lauro E., S. De Martino, M. Palo, and J.M. Ibañez (2010), Self–sustained oscillations at Volcán de Colima (México) inferred by Independent Component Analysis, *submitted to Geophysical Journal International*.

De Martino S., M. Falanga and C. Godano (2004), Dynamical similarity of explosions at Stromboli volcano, *Geophys. J. Int., 157(3)*, 1247-1254.

De Martino S., M. Falanga, M. Palo, P. Montalto, D. Patané (2010), Statistical analysis of the seismicity during the Strombolian crisis of 2007, Italy: evidence of a precursor in the tidal range, *submitted to Journal of Geophysical Research.*. The submitted manuscript is available on the website http://hdl.handle.net/2122/6150.

Dietel C., B.A. Chouet, J. Kleinman, G. De Luca, M. Martini, J. Power, D. Harlow and R. Scarpa (1994), Array tracking tremor sources at Stromboli volcano, Italy, U.S. Geol. Surv., Open-File Rep. 94–142, 1–86.

Fiori S. (2003), Overview of independent component analysis technique with an application to synthetic aperture radar (SAR) imagery processing, *Neural Net.,16*,453-467.

Fletcher N. H. (1999), The nonlinear physics of musical instruments, *Rep. Prog. Phys.,62*,723-764.

Goldstein, P. and R. J. Archuleta (1987), Array analysis of seismic signals, *Geophys. Res. Lett., 14*,1,13-16, doi:10.1029/GL014i001p00013.

Harris D. B. (1991), A waveform correlation method for identifying quarry explosions, *Bull. Seism. Soc. Am., 81*, 6,2395-2418.

Hellweg M. (2003), The polarization of volcanic seismic signals: medium or source?, *J. Volcanol. Geotherm. Res., 128*, 159-176.

Hyvarinen A. and E. Oja (2000), Independent component analysis: algorithms and applications. *Neural. Net.,13*, 411-430.

Hyvärinen, A., Karhunen, J.Oja, E., (2001), *Independent Component Analysis*, John Wiley and Sons, New York.

Landi P., R.A. Corsaro, L. Francalanci, L. Civetta, L. Miraglia, M. Pompilio, R. Tesoro (2009), Magma dynamics during the 2007 Stromboli eruption (Aeolian Islands, Italy): mineralogical, geochemical and isotopic data, *J. Volcanol. Geotherm. Res., 182*, 255-268, doi:10.1016/j.jvolgeores.2008.11.010.

La Rocca M., S. Petrosino, G. Saccorotti, M. Simini, J. Ibañez, J. Almendros and E. Del Pezzo (2000), Location of the source and shallow velocity model deduced from the explosion quakes recorded by two seismic antennas at Stromboli volcano, *Phys. Chem. Earth (A), 25*, (9-11), 731-735.

Martini, M., L. D′Auria, T. Caputo, F. Giudicepietro, R. Peluso, A. Caputo, W. De Cesare, A.M. Esposito, M. Orazi, and G. Scarpato (2008), Seismological insights on the shallow magma system, in *The Stromboli Volcano: An integrated study of the 2002–2003 Eruption*, S. Calvari, S. Inguaggiato, G. Puglisi, M. Ripepe, and M. Rosi eds., AGU Geophysical Monograph Series, 182, 279–286.

Marzocchi, W. and L. Zaccarelli (2006), A quantitative model for the timesize distribution of eruptions. *J. Geophys. Res., 111*, B04204.

Palo, M., E. De Lauro, S. De Martino, M. Falanga, G. B. Cimini (2010), Statistical properties of explosions during the last two eruptions at Stromboli volcano, Italy, *Geophysical Research Abstracts, 12*, EGU2010–8913, EGU General Assembly 2010.

Pino, N.A., M. Ripepe, and G.B. Cimini (2004), The Stromboli Volcano landslides of December 2002: A seismological description, *Geophys. Res. Lett., 31*, L02605, doi:10.1029/2003GL018385.

Scandone, R., F. Barberi, and M. Rosi (2009), The 2007 eruption of Stromboli: Preface, *J. Volc. Geoth. Res., 182*, v, doi:10.1016/j.jvolgeores.2008.12.019.

Tinti, S., A. Manucci, A. Pagnoni, A. Armigliato, and F. Zaniboni (2005), The 30 december 2002 landslide-induced tsunamis in Stromboli: sequence of events reconstructed from the eyewitness accounts, *Nat. Hazards. Earth Syst. Sci., 5*, 763–775.

Vergniolle, S., G. Brandeis, and J.-C. Mareschal (1996), Strombolian explosions: 2. Eruption dynamics determined from acoustic measurements, *J. Geophys. Res., 101(B9)*, 20,44920,466.

Figure 1. Map of Stromboli island. The positions of the crater area and the seismic station (SX15) are emphasized by the red circles.

Figure 2. Example of the explosion detection method applied on 35 minutes of signal starting on 17/07/2002 h 15.32.22. The stars mark the detected explosions.

Figure 3. Time-evolution of the spectral content of the explosions. We estimate the amplitude spectra of each explosion and normalize them singularly with respect to the maximum of each spectra. Then, we average the normalized spectra of 300 successive explosions. These averaged spectra are represented as a spectrogram. The scale of the color is chosen to optimize the visualization of the spectral changes. The time scale in not uniform because the number of events changes along the data-set. We distinguish four different spectral classes labelled as Phase A, B, C, D, respectively (see the text for the details of each phase). Phase B includes the basic spectral content, showing principal peaks at about 1, 2, 3 Hz. Since the end of September 2002 until the crisis onset these principal spectral peaks increase in amplitude and high-frequency modes (4, 5 Hz) emerge, suggesting that an energy enhancement is occurring.

Figure 4. Mean normalized amplitude spectra. We show four representative cases calculated as the mean spectra of the explosions occurring in the periods a) 13-30/07/2002 (Phase A); b) 6-23/10/2002 (Phase B); c) 10-14/01/2003 (Phase C, that is during the crisis); d) 25/11/2002 (Phase D).

Figure 5. Typical explosion waveforms for the four classes recognized on the basis of the spectral analysis. a) Phase A (22/07/2002 h. 04.26); Phase B (27/10/2002 h. 15.13); Phase C (10/01/2003 h. 06.16); Phase D (17/11/2002 h. 16.35).

Figure 6. Information retained as function of the number of the principal components. It has been estimated by computing the diagonalization of the covariance matrix composed of 20 consecutive explosions and calculating the ratio between the sum of the first N eigenvalues and that of all the eigenvalues. The results are averaged over all the groups of 20 explosions.

Figure 7. Independent components in time and frequency domain. The independent components are indicated on the top of the panels on the left. The amplitudes of the signals (and, hence, those of the respective spectra) are not comparable because ICA provides only the waveform of the independent components, but not the energy. Transient independent components (IC4 and IC5) have been extracted analyzing, respectively, the Phase C and the Phase A of the data-set.

Table 1. a) Frequency peak of the time-stable and transient independent components. b) Frequency bands adopted to identify the ICs in the original signals.

	(a) frequency peak (Hz)	(b) frequency bands (Hz)
IC1	1.1	(1.0-1.5)
IC2	1.8	(1.6-2.2)
IC3	2.5	(2.3-2.7)
IC4	0.3-0.4	(0.2-0.5)
IC5	5	(4-6)

Figure 8. Waveform of the explosion recorded on 03/08/2002 h. 20.32 (North-South component) and time-evolution of the corresponding polarization parameters. The signal is frequency filtered in the range 1.1-2.7 Hz to contain the three time-stable ICs. The solutions oscillate around a value, as occurs when only a single seismic phase is present.

Figure 9. Distributions of the polarization parameters averaged over all the explosions. Only high-RL solutions have been selected. Frequency of the solutions is expressed as a probability. The scattering of the medium leads to the dispersion of the solutions and the particle motion becomes very shallow when the frequency increases.

Figure 10. (a) Time-evolution of mean value and standard deviation (plotted as error-bars) of energy computed in non-overlapping time-windows of 12 hours. Energy is in log-scale. The red vertical line indicates the crisis onset. The two green lines and the red line separate the four time-intervals cited in the text and labelled as Phase I-II-III-IV, respectively. Over these time-intervals we have computed the distributions of Fig. 11. The dashed blue lines represent the edges of the Phases A-B-C-D previously introduced on the basis of the spectral content. The time-interval of the Phase C coincides with that of the Phase IV; (b) Time-evolution of the variability coefficient estimated in sliding and non-overlapping windows of 8 hours; (c) Occurrence rate estimated as the inverse of the mean inter-time in non-overlapping windows of 3 hours. Swarms are detected when the occurrence rate exceeds λ_t (represented by the dashed horizontal line.)

Figure 11. Energy distribution estimated in four disjoined time-intervals indicated at the top of the panels and corresponding, respectively, to the Phase I, II, III, IV. Phase I, II, III include three sectors of 60-80 days spanning from the start of recordings to the crisis onset; Phase IV includes about one month after the crisis onset. Frequency of the solutions is expressed as a probability. Energy is measured in log-scale.

Figure 12. Examples of two swarm's explosions in time and frequency domain recorded on 06/01/03 h. 10.20 (panel a,b) and on 19/01/03 h. 20.31 (c,d).

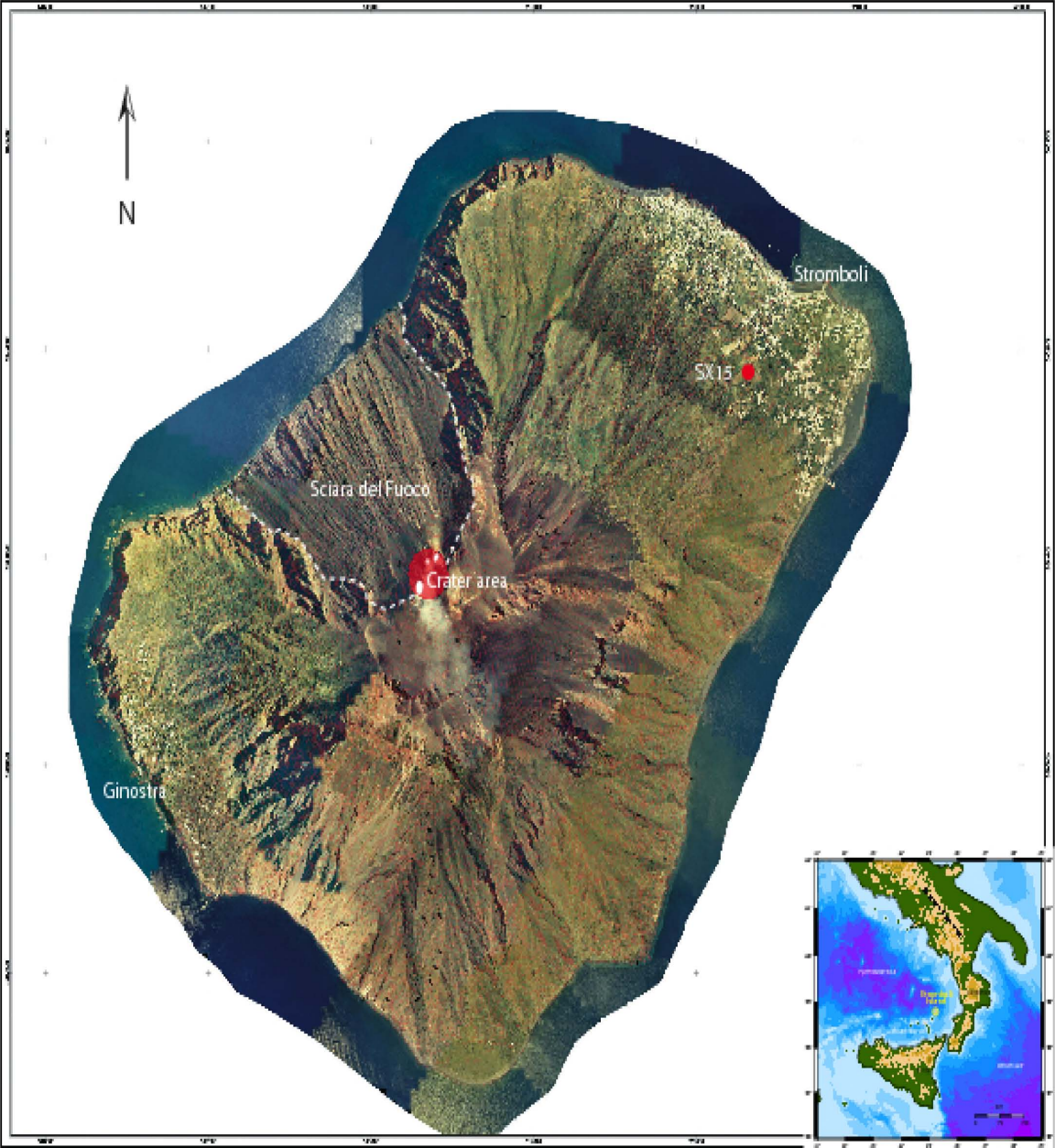
N
Stromboli
SX15
Sciara del Fuoco
Crater area
Ginostra

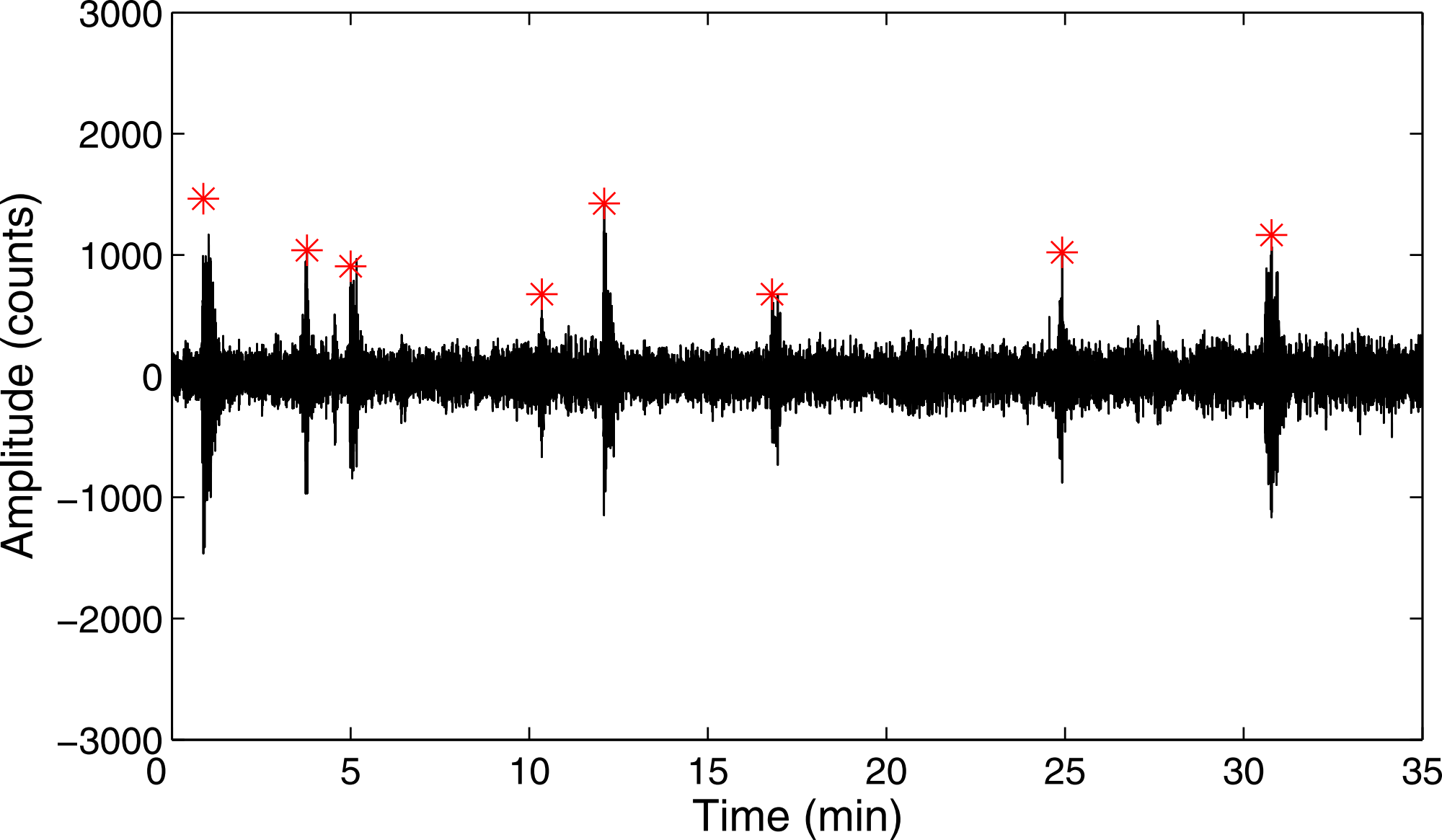
3000
2000
1000
0
−1000
−2000
−3000
Amplitude (counts)
0
5
10
15
20
25
30
35
Time (min)

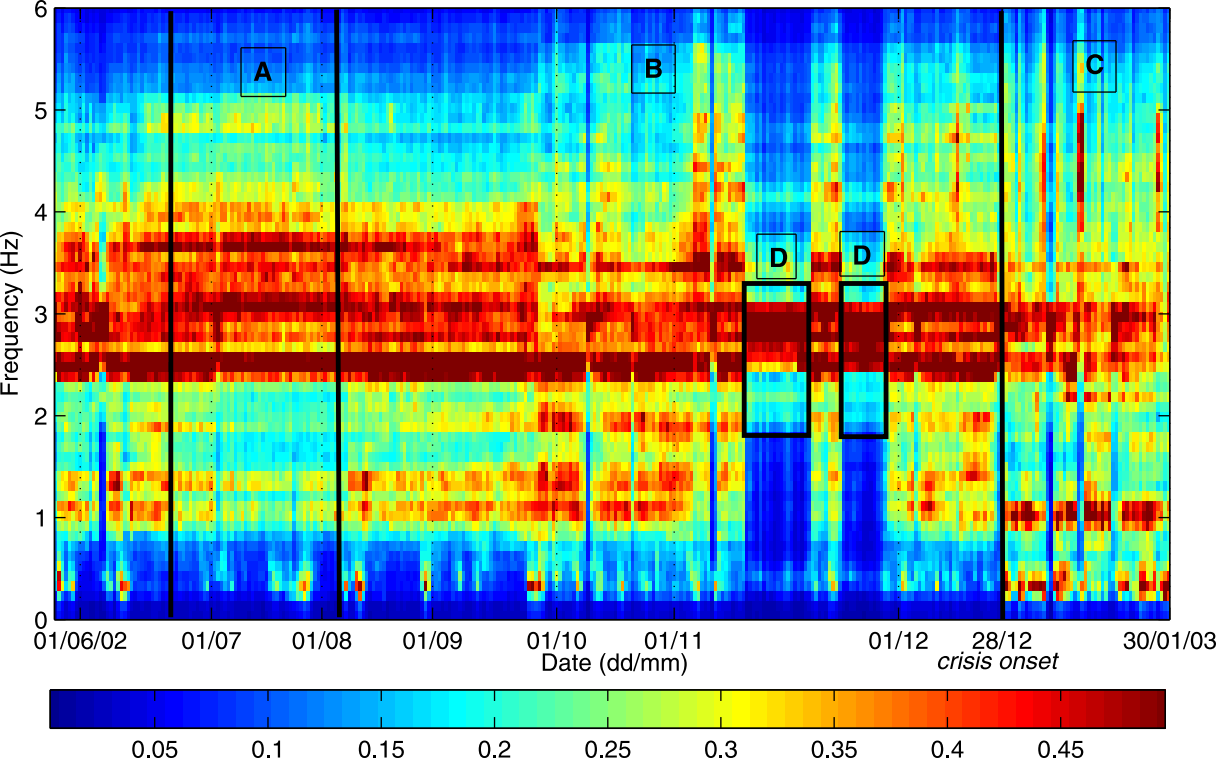
A
B
C
D
D
Frequency (Hz)
0
1
2
3
4
5
6
01/06/02
01/07
01/08
01/09
01/10
01/11
01/12
28/12
30/01/03
Date (dd/mm)
crisis onset
0.05
0.1
0.15
0.2
0.25
0.3
0.35
0.4
0.45

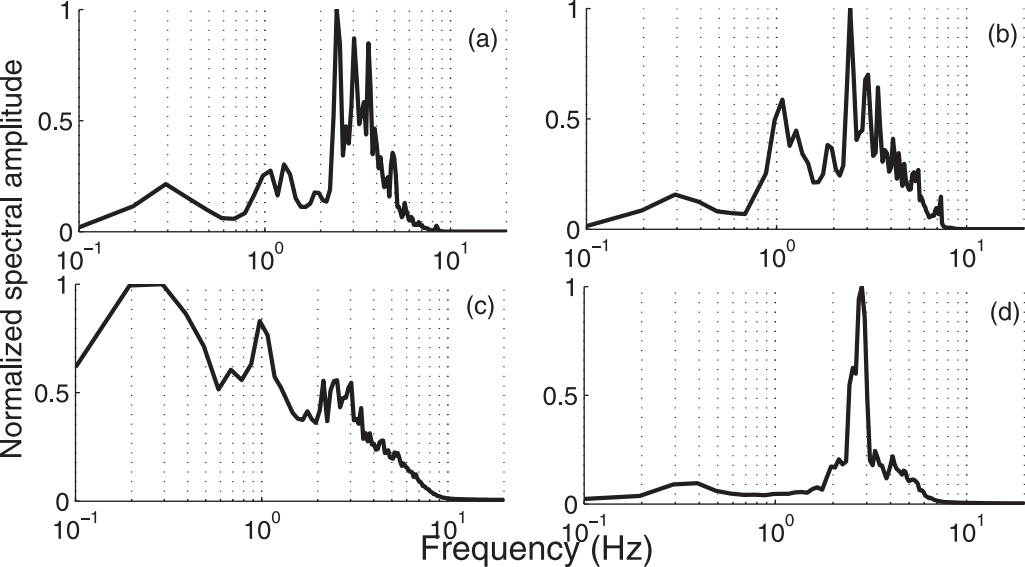
(a)
(b)
(c)
(d)
Normalized spectral amplitude
Frequency (Hz)
0
0.5
1
10^{-1}
10^{0}
10^{1}

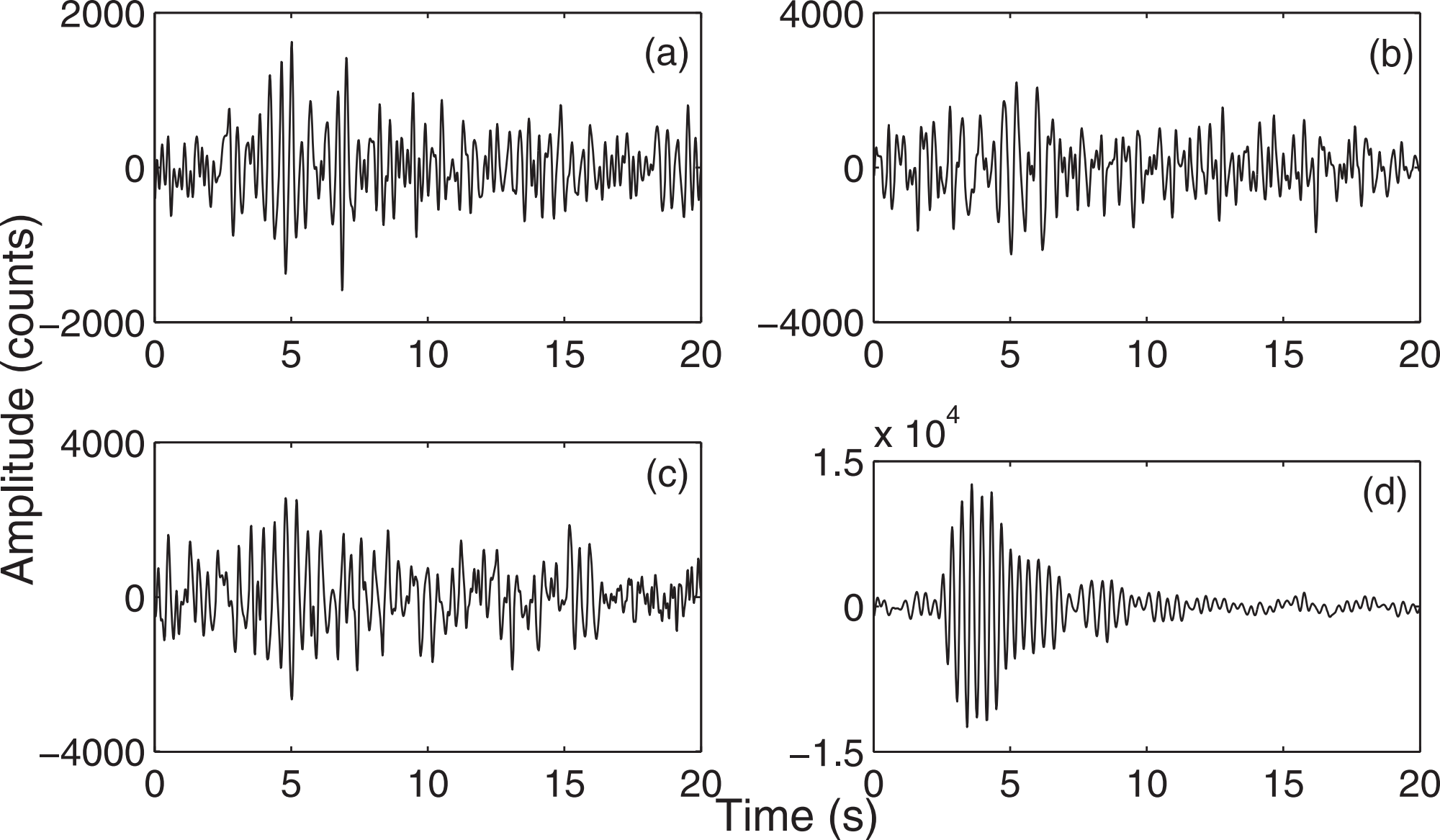
(a)
(b)
(c)
(d)
2000
0
−2000
4000
−4000
1.5
−1.5
x 10^4
0
5
10
15
20
Amplitude (counts)
Time (s)

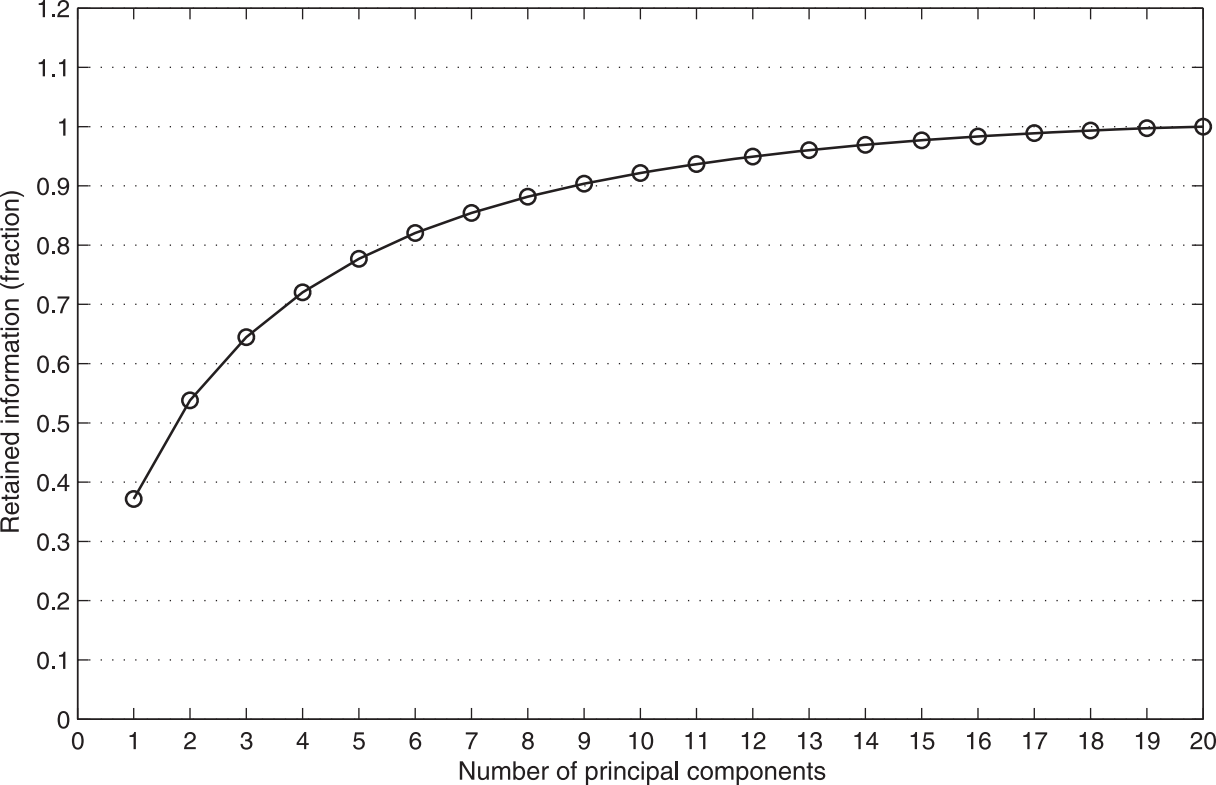
Retained information (fraction)
Number of principal components
0
0.1
0.2
0.3
0.4
0.5
0.6
0.7
0.8
0.9
1
1.1
1.2
0 1 2 3 4 5 6 7 8 9 10 11 12 13 14 15 16 17 18 19 20

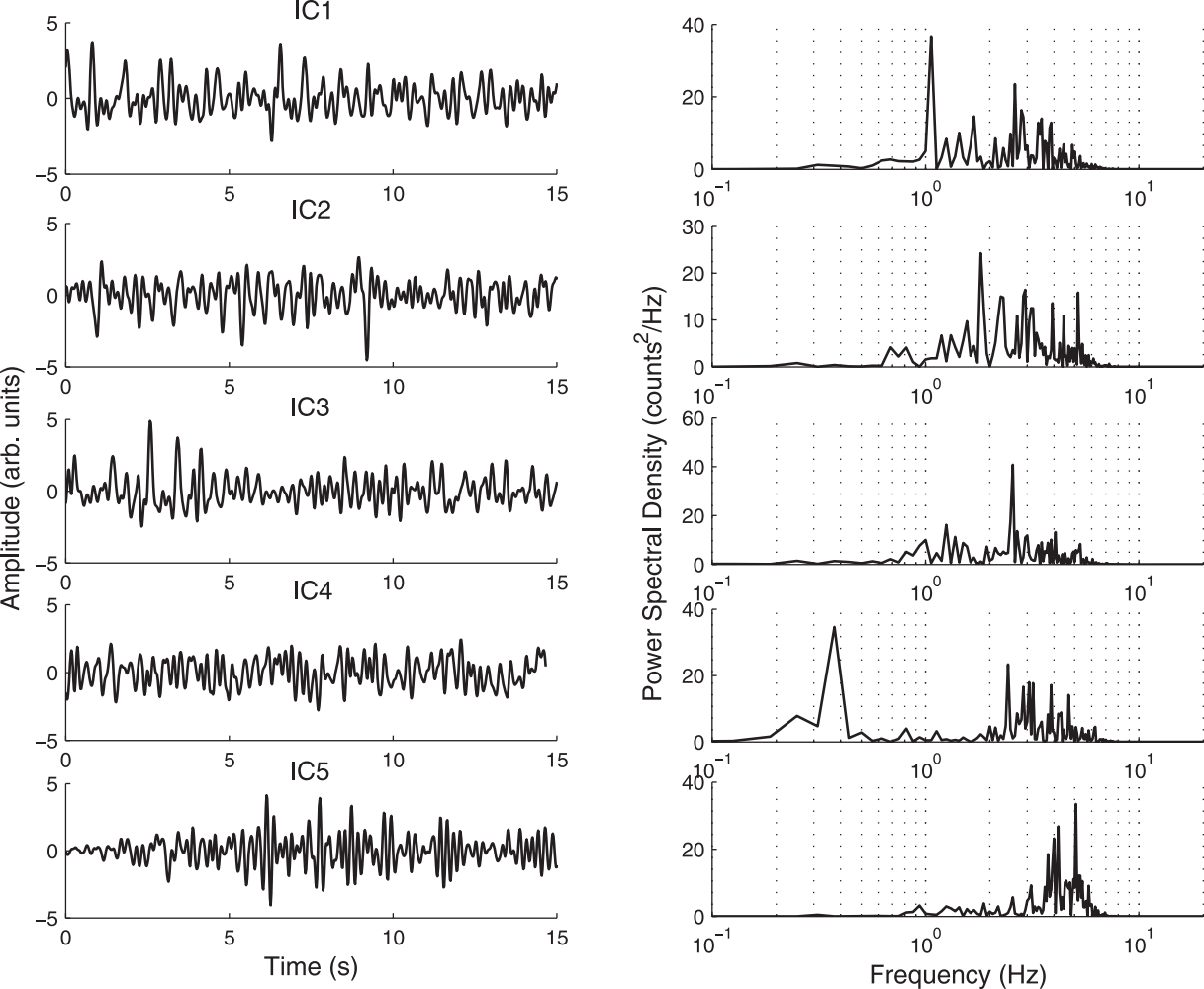
IC1
IC2
IC3
IC4
IC5
Amplitude (arb. units)
Time (s)
Power Spectral Density (counts^2/Hz)
Frequency (Hz)

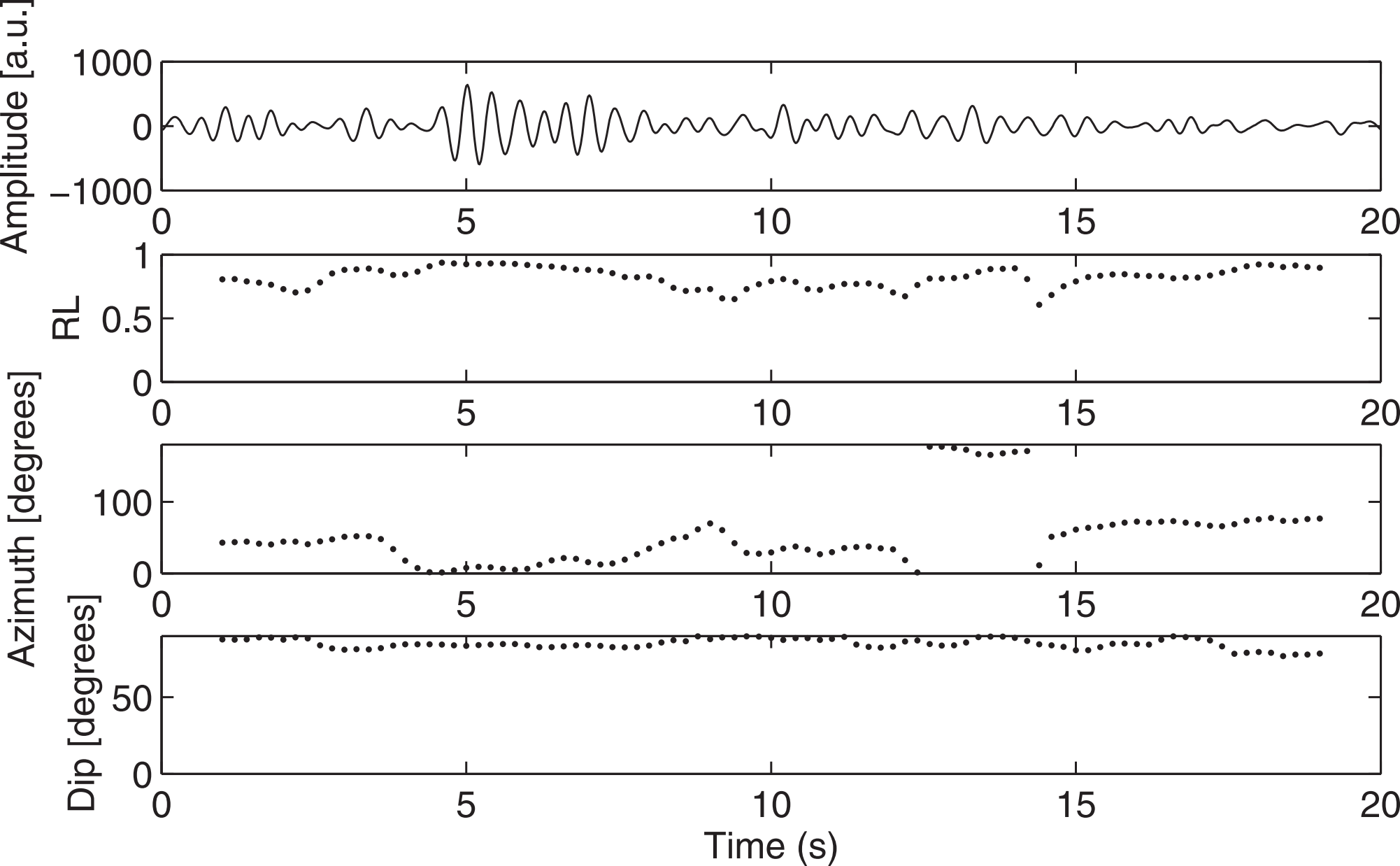
Amplitude [a.u.]
1000
0
−1000
0
5
10
15
20
RL
1
0.5
0
Azimuth [degrees]
100
0
Dip [degrees]
50
Time (s)

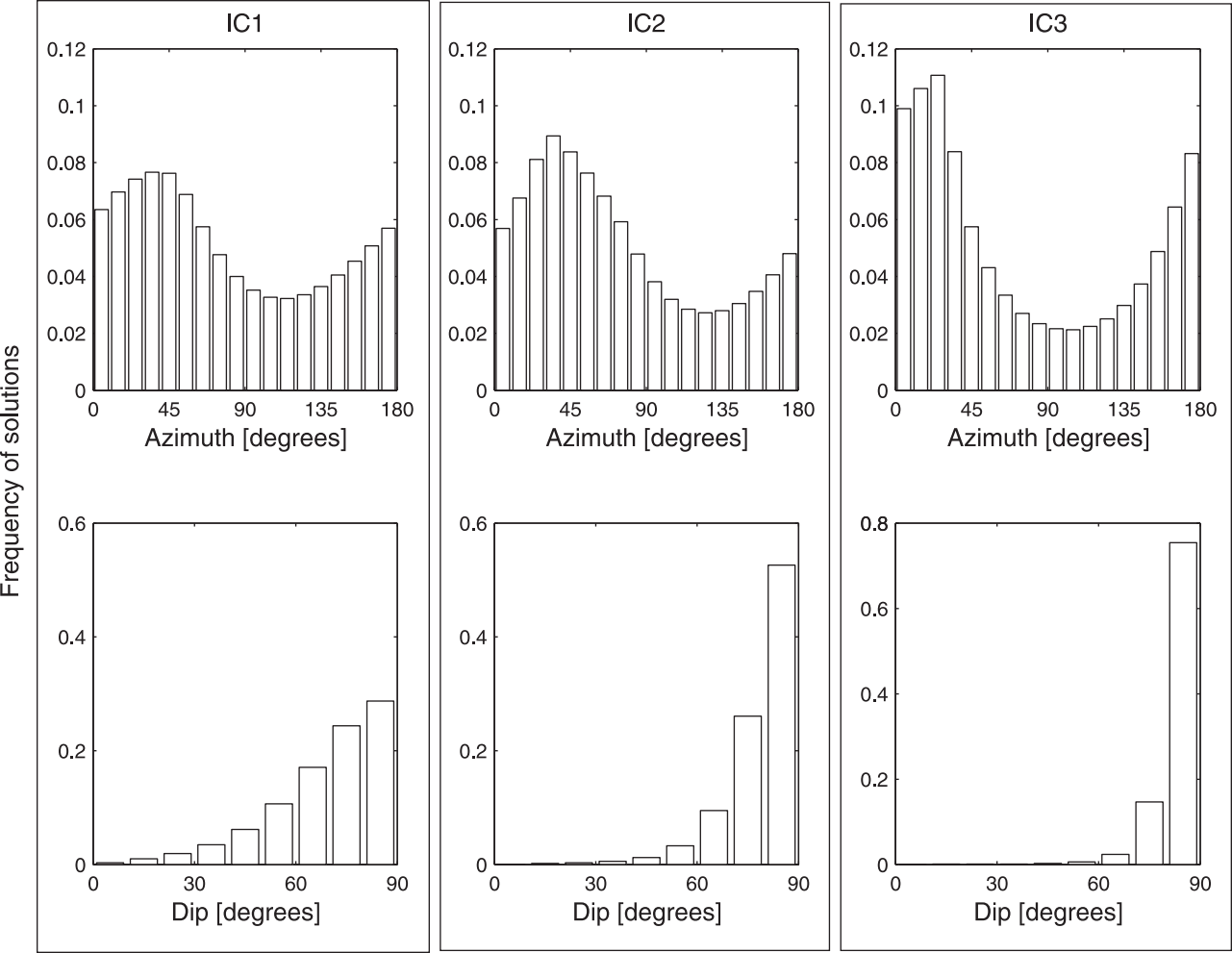
IC1
IC2
IC3
Frequency of solutions
Azimuth [degrees]
Dip [degrees]
0.12
0.1
0.08
0.06
0.04
0.02
0
0.6
0.4
0.2
0.8
0
45
90
135
180
30
60

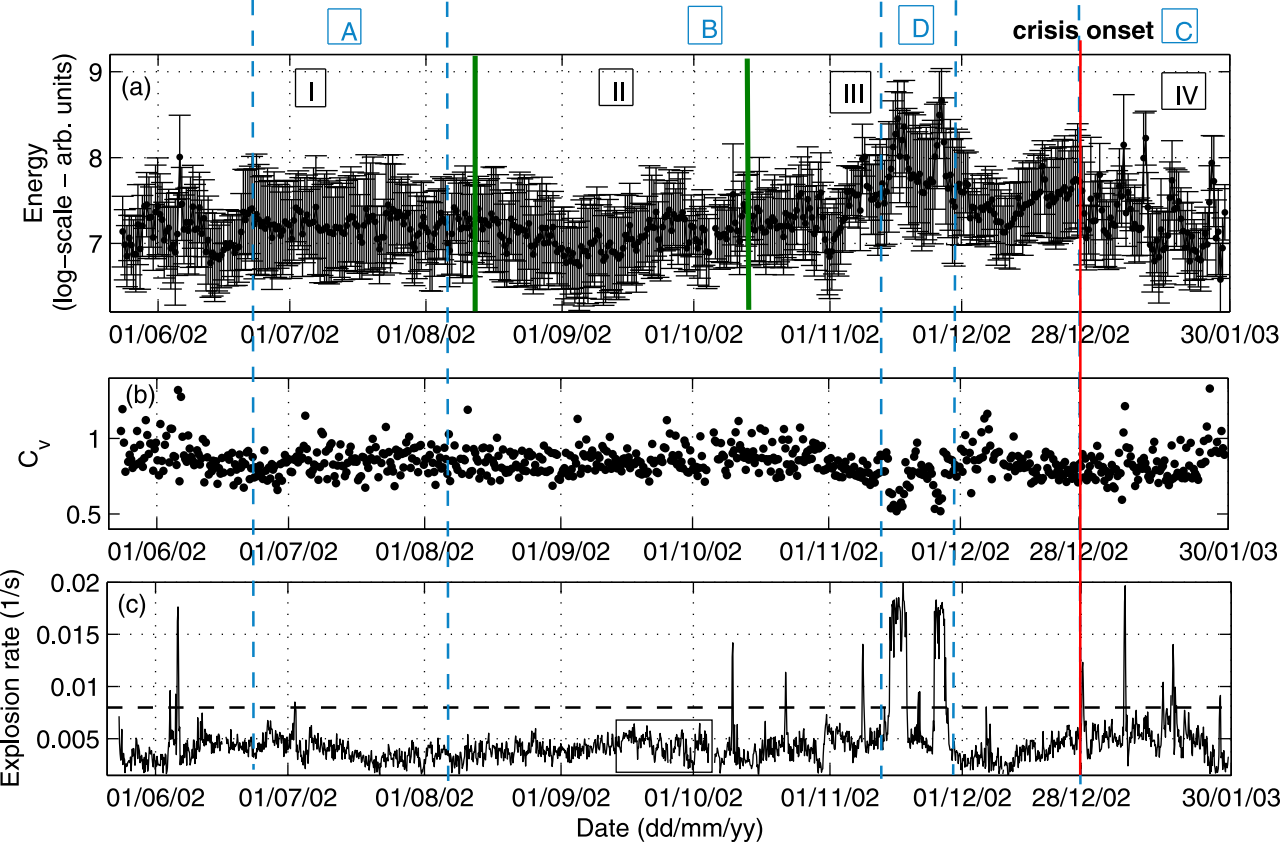
A
B
D
crisis onset
C
(a)
I
II
III
IV
Energy
(log–scale – arb. units)
9
8
7
01/06/02
01/07/02
01/08/02
01/09/02
01/10/02
01/11/02
01/12/02
28/12/02
30/01/03
(b)
C_v
1
0.5
(c)
Explosion rate (1/s)
0.02
0.015
0.01
0.005
Date (dd/mm/yy)

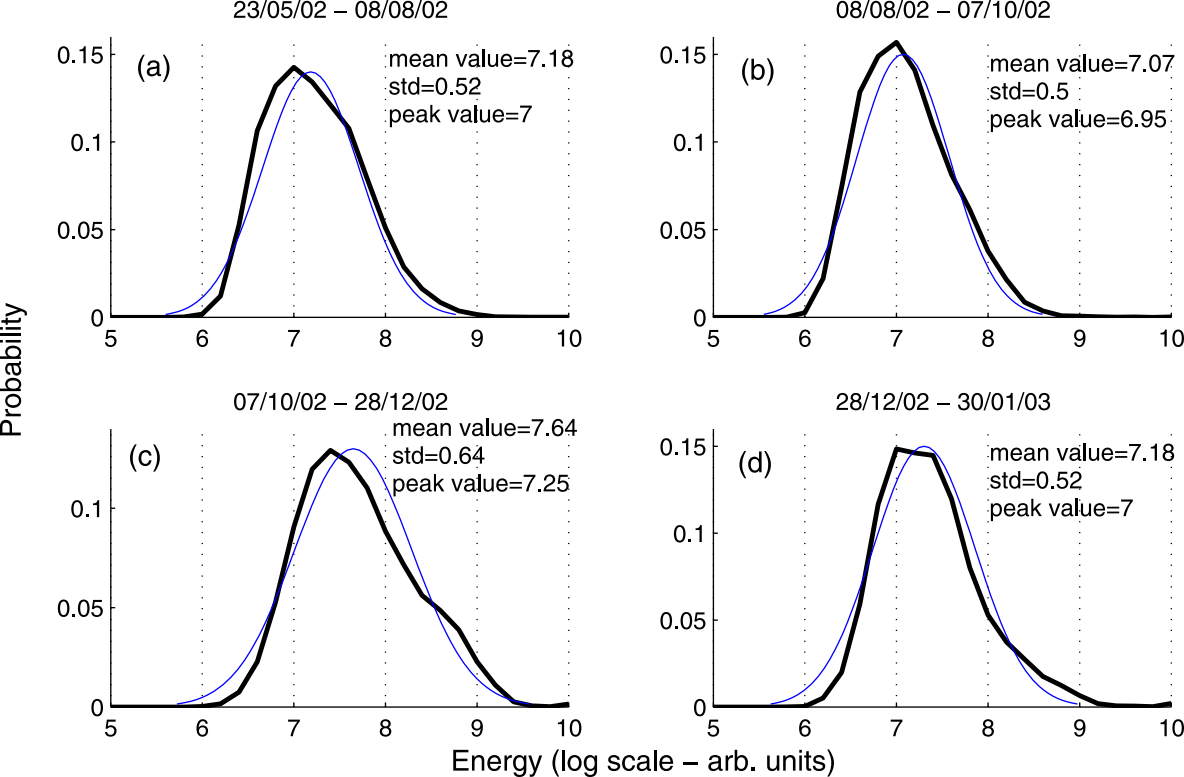
23/05/02 – 08/08/02
(a)
mean value=7.18
std=0.52
peak value=7
08/08/02 – 07/10/02
(b)
mean value=7.07
std=0.5
peak value=6.95
07/10/02 – 28/12/02
(c)
mean value=7.64
std=0.64
peak value=7.25
28/12/02 – 30/01/03
(d)
mean value=7.18
std=0.52
peak value=7
Probability
Energy (log scale – arb. units)

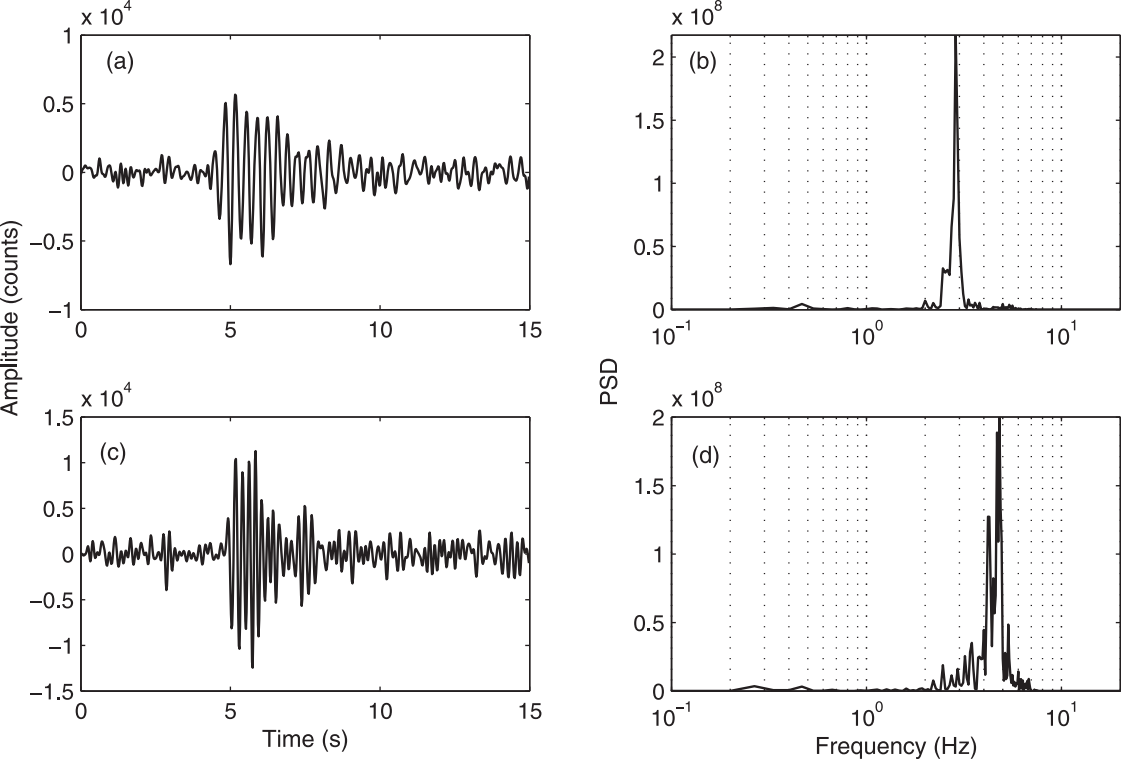
x 10^4
(a)
1
0.5
0
−0.5
−1
0
5
10
15
Amplitude (counts)
x 10^8
(b)
2
1.5
1
0.5
0
10^−1
10^0
10^1
PSD
x 10^4
(c)
1.5
1
0.5
0
−0.5
−1
−1.5
0
5
10
15
Time (s)
x 10^8
(d)
2
1.5
1
0.5
0
10^−1
10^0
10^1
Frequency (Hz)